X-ray preconditioning for enhancing refractive index contrast in femtosecond laser photoinscription of embedded waveguides in pure silica

Maxime Royon, Emmanuel Marin, Sylvain Girard, Aziz Boukenter, Youcef Ouerdane, Razvan Stoian

Research Article | Vol. 9, No. 1 | 1 Jan 2019 | OPTICAL MATERIALS EXPRESS 65

Optical Materials EXPRESS

X-ray preconditioning for enhancing refractive index contrast in femtosecond laser photoinscription of embedded waveguides in pure silica

MAXIME ROYON,* EMMANUEL MARIN, SYLVAIN GIRARD, AZIZ BOUKENTER, YOUCEF OUERDANE, AND RAZVAN STOIAN

Laboratoire Hubert Curien, CNRS UMR5516, Université de Lyon, Université Jean Monnet, F-42023, Saint-Etienne, France
**maxime.royon@univ-st-etienne.fr*

Abstract: We investigate femtosecond pulse laser-induced refractive index changes (Δn) in bulk fused silica (Corning 7980) subject to prior hard (40 keV) X-ray irradiation with accumulated doses up to 6 MGy. The preconditioning before photoinscription improves strongly the light transport of the laser-written embedded waveguides in a range of fluences and accumulation doses. Results show that the ultrafast laser-induced Δn is higher in samples pre-irradiated with X-rays at similar laser photon dose. The effect lies in the kick-off generation of defects and precursors by energetic X-ray photons, enhancing a subsequent laser-induced densification process. The photoinscription efficiency increases up to a saturation point and the pre-treatment can be considered as an effective option for high contrast low loss index modifications and waveguiding structures in glasses.

1. Introduction

Nowadays, ultrafast lasers are promising tools for 3D structuring of optical materials, enabling the design of stable and compact devices for integrated photonic applications. The strong energy concentrations achievable via focused ultrashort pulses and the flexibility in irradiation geometry leads to permanent structural changes and refractive index variations in three-dimensional arrangements [1]. For a model glass, such as pure fused silica, the typical intensity ranges for photoinscription allow for tuning index changes from isotropic soft positive index changes (Type I) to strong negative rarefaction-driven index variations (Type II) [2]. The first interaction regime is typically used for guiding applications, in embedded optics and 3D photonics, with typical index contrast in the range of 10^{-3} and losses below 1 dB/cm. The contrast of the refractive index changes in ultrafast laser volume photoinscription of optical materials is nevertheless a key issue in device performance. Particularly for waveguiding applications, it allows to control modal dimensions [2], bending losses [3], or evanescent coupling [4]. A present challenge of the ultrafast laser photoinscription technique is therefore the increase of the index contrast fostering better performances of the devices. The typical structural scenario involved in generating Type I index changes relies on a defect-driven densification path [5,6]. Building up on this hypothesis, we explore here ways of prior conditioning of materials for developing an incipient defect density. This is meant to subsequently serve as precursors for enhanced photoinscription efficiency and a higher index change. We discuss therefore here material treatment conditions via X-ray irradiation in fused silica glasses and explore the effects in different structural rearrangements and defect-driven densification scenarios. The question we have tried to answer is if a preconditioning of the materials in terms of defect accumulation can modify the efficiency of the ultrafast laser photoinscription process and result in higher index contrast. Indeed, the photo-inscription of 3D components with a more or less exotic architecture can become a very time-consuming

#344968 https://doi.org/10.1364/OME.9.000065
Journal © 2019 Received 5 Sep 2018; revised 22 Oct 2018; accepted 27 Oct 2018; published 5 Dec 2018

Optical Materials EXPRESS

process so as to achieve the best performances regarding the refractive index change. We will demonstrate the beneficial effect on the magnitude of the femtosecond laser induced index change using Raman and photoluminescence (PL) spectroscopy and we will attempt to deliver an explanatory mechanism based on structural changes related to defects.

2. Experimental description

We have used high purity Corning 7980 silica (20x10x5 mm^3) polished samples for our experiments, a synthetic silica glass produced by hydrolysis of $SiCl_4$ when fused by a H_2/O_2 flame. According to Brückner classification, it is a wet silica type since it is characterized by a high concentration of OH groups (about 800-1000 ppm) [7]. Moreover, this glass does not possess metallic impurities but it can contain small traces of Cl (less than 1 ppm). Before exposure to femtosecond laser pulses, several samples were pre-irradiated with X-rays at different accumulated doses of 6 MGy (SiO_2), 1 MGy and 0.5 MGy with a dose rate of 63 Gy/s. Main energy of the X-rays is 40 keV.

The refractive index modifications inside the bulk samples were performed by a regeneratively amplified Ti:Sapphire femtosecond laser (Coherent RegA) operating at 800 nm with a pulse duration of 150 fs (FWHM) and a 100 kHz repetition rate. The power was adjusted using a polarizer and a half wave plate and the beam was focused through a long working distance 20x plan apochromatic objective (NA = 0.42). A computer controlled XYZ stage (Aerotech ANT-130-5-V and ANT-130-060-XY) was used in order to translate the samples with respect to the focal volume. As we work in a transverse writing configuration, the intensity distribution of the focused beam is elongated along the propagation axis in the confocal region. To obtain a circular form and optimize the waveguide cross section, we used the slit beam shaping technique [8]. In the present experiments, the incident beam was clipped by a 450 µm slit before the microscope objective. Under this condition, by scanning the shaped focused beam in our configuration, a cylindrical waveguide of 10-12 µm diameter can be photo-inscribed. Pulse energies, measured after the slit, from 1.2 µJ to 1.7 µJ and translation speeds between 100 µm/s and 600 µm/s with 8 passes were chosen to photo-inscribe waveguides. It is to note that the high energy range required to obtain Type I modifications compared to classical conditions is justified by the slit-shaped beam that distributes the energy on a larger section. All the waveguides presented in this work are written 150 µm below the polished silica surface with a 10 mm length.

A white light source (350-2000 nm) was used to inject light into the waveguides in order to evaluate their guiding properties. The Δn was determined through the measurements of the Numerical Aperture (NA) of the output light projected in far-field on a CMOS camera (Thorlabs DCC1645C). In addition, relative index contrast was measured via positive Phase Contrast Microscopy (PCM).

In order to investigate the point defects and the local structural changes that appear in the process of refractive index variation, we have made photoluminescence (PL) and Raman spectroscopy measurements with an integrated confocal microRaman ARAMIS (Horiba Jobin-Yvon) in a backscattering configuration using a 325 nm (3.81 eV) He-Cd laser as excitation probe light. The laser beam was focused into the waveguides by a 40x UV objective and the samples were mounted on a XYZ controlled stage with a micrometric precision. The spatial resolution was fixed at 4.6 µm through a confocal pinhole diameter of 75 µm.

3. Results and discussions

3.1 Correlation between the NBOHC yield and Δn

The results presented below are to be understood in a perspective of a defect-assisted densification process. Let us first briefly review the physical processes involved in the laser induced refractive index at near-infrared wavelengths and short pulse durations. Due to the

Optical Materials EXPRESS

relatively strong laser intensity approaching the TW/cm^2 level, the multiphoton ionization process in transparent material allows the promotion of an electron to the conduction band, leaving a hole in the valence band. If the resulting carrier density is significantly smaller than the critical density, the matrix retains a rigid character and the relaxation proceeds via a strong interaction between the free carrier and the polarizable molecular environment. Consequently, a free carrier trapping occurs, also known as Self-Trapped Excitons (STE's) relaxation, leading to Si-O bond breaking and the formation of the well known paramagnetic defects: Non-bridging-Oxygen-Hole-Centers (NBOHC) and E' centers [9]. Alternatively, the link may be reformed, closing the molecular -Si-O- rings. The consequence of this Si-O bond breakup is thus an opportunity for structural and electronic reorganization. It is then worth noting that the network reorganization will potentially results into formation of smaller rings (material densification) [10,11]. Thus the generation of electronic defects and the structural densification are the two correlated facets of the phenomenon of bond breaking, with a part being transformed in color centers, stabilizing the bond break-up and other part being reformed in other more compacted structural arrangements. The idea of a densification assisted by defects has been described in the literature [12,13] and results concerning molecular dynamics on glass samples containing a large defect density showed and confirmed a change in ring statistics and a decreasing in the interbonding angle Si-O-Si, both leading to a density increase [14,15].This densification, being a function of the defect density, induces a smooth and isotropic refractive index change (Type I) allowing light guiding in the laser written structures. The structural nature explains equally the preservation of the index contrast at annealing temperatures typically erasing the electronic defects. Thermally-induced refractive index changes are thus not discussed, except to indicate the onset of thermomechanical rarefaction generating low index Type II structures. Concerning this latter aspect, Type I modifications are determined by bond breaking and structural reorganization and seem not to be heat or fictive temperature (T_f) driven, as the achievable level of temperature under regular processing conditions stays low. Calculations considering nonlinear pulse propagation [16,17] indicate that, when considering electron light scattering and plasma defocusing, the increase of temperature after a single pulse is well below the softening value. At this level, heat driven structural reorganization cannot happen on the μs duration of the thermomechanical cycle. Based on this argument, we emphasize the dominant role of bond breaking in the structural reorganization process, giving the frame for the subsequent discussion.

Optical Materials EXPRESS

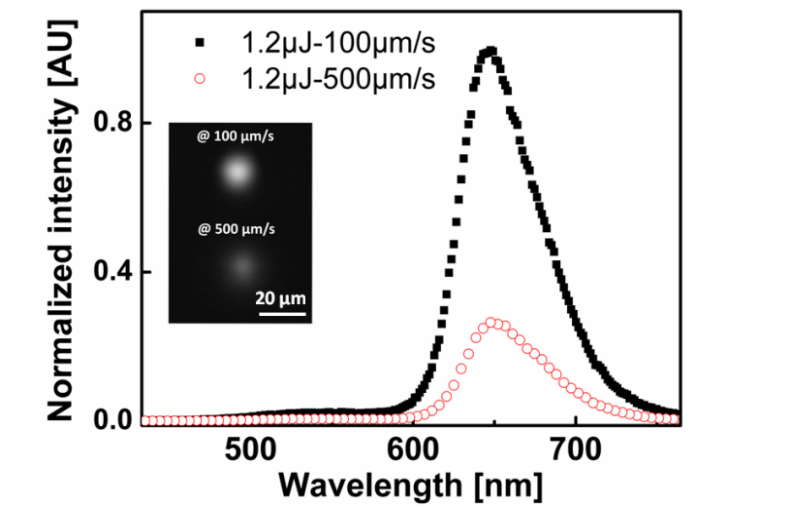

Fig. 1. Luminescence of NBOHC excited at 325 nm inside two waveguides written with ultrashort laser pulses at fixed pulse energy (1.2 µJ) and two different scanning speeds (100 µm/s and 500 µm/s). The inset shows the corresponding large-band guided modes.

In Fig. 1, a PL measurement recorded inside two different waveguides written in a pristine sample is shown. We can see the presence of a 650 nm (1.9 eV) emission band if excited with 325 nm laser radiation, indicating the formation of NBOHC [18] after exposure to femtosecond laser pulses. This well-known emission band has been studied since a long time and is observed when silica glasses are irradiated with X-rays, γ-rays, UV lasers or even neutrons [19]. Furthermore, the yield of this emission band depends on the photon dose used for generating the modification. With respect to the waveguide written with the highest light dose (i.e 1.2µJ-100 µm/s), we have a relatively high NBOHC concentration alongside favorable guiding properties in terms of mode confinement, implying an important Δn. However, PL measurements recorded inside the waveguide photo inscribed with a lower dose (1.2µJ-500 µm/s) reveal a decrease in the NBOHC content. The corresponding guided mode confirms a poorer Δn compared with the previous one. We retain thus a correlation between the PL NBOHC yield and the ultrafast laser induced Δn, hence with the amount of densification. It is to be noted here that low temperature (T<400 K) treatment can anneal the defects but preserve the index change [20].

3.2 Effect of X-ray irradiation in the bulk silica glass

The idea of pre-irradiation is the potential generation of precursors for further laser-induced defect generation, as well as an overall increase in photosensitivity. X-rays are ideal tools for generating defects by kick-off mechanisms, and preconditioning by irradiation can validate fundamentally the bond-breaking densification scenario. In order to validate the benefit of a preconditioning in term of defect accumulation on the refractive index change, we have irradiated samples with different X-rays accumulated dose before exposure to femtosecond laser beam. The primary effect of X-rays irradiation is a suite of bond breaking events and Fig. 2 displays the concentration of NBOHC after X-rays treatment as a function of the depth in the sample for different accumulated doses, mapping the stopping power. In the pristine sample (no X-rays irradiation), no NBOHC are observed. However, even with the lowest 0.5 MGy dose, the sample exhibits a low content of NBOHC. In the inset of Fig. 2, we can clearly see a saturation effect at higher doses, measured in the spatial region where the waveguides will be written (150 µm) with ultrashort laser pulses. It is important to note that in all the X-rays preconditioned samples, only NBOHC are observed, whatever the accumulated dose, in the spectral range used in this experiment for the PL characterization

Optical Materials EXPRESS

(400 nm-800 nm). The fact that the NBOHC distribution is not homogeneous within the bulk glass is explained by the penetration efficiency of the used X-rays with energy of roughly 40 keV, that are mainly stopped in the first half mm inside the sample. However, with 1 MeV γ-rays, a homogeneous NBOHC distribution is expected, and a similar laser induced Δn could be achieved along the entire sample.

Furthermore, the Raman spectra obtained in the bulk of the X-rays pre-irradiated samples (recorded close to the surface at a depth of ~20 µm) have shown that there is no appreciable structural changes in term of densification even with the maximum accumulated doses of 6 MGy used in this experiment.

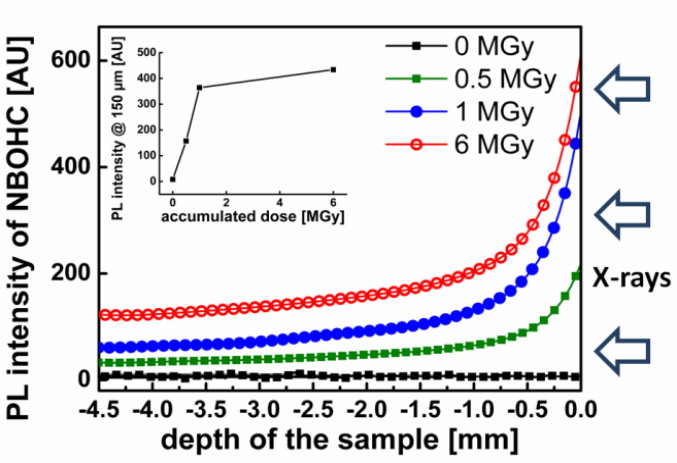

Fig. 2. Relative concentration of X-ray induced NBOHC in fused silica mapped via the characteristic PL as a function of the depth of the sample for different doses of X-rays that are stopped in the first half mm. The inset shows the PL intensity of NBOHC recorded at a depth of 150 µm as a function of the accumulated dose.

Depending on the irradiation source, other point defect can be induced. Indeed, the literature shows that electron irradiation (2.5 MeV) of pre-densified bulk silica glasses reveals the presence of NBOHC and the presence of another defect associated to a PL band peaking at 540 nm [21] whose origin is still unclear. This green luminescence is also observed in bulk silica glass when irradiated with UV laser [22]. However, in our experiment, this unattributed band is not observed after X-rays irradiation.

3.3 Waveguide analysis

Ultrafast laser index modification traces are then written in the preconditioned samples in similar conditions as those given in Fig. 1. These structures were investigated from a structural and light guiding perspective.

First, after the laser photoinscription process, the corresponding Raman spectra of the waveguides written in the pristine and pre-treated samples are investigated. In Fig. 3(a), we report the comparison between the Raman spectra of three different waveguides written in the pristine and X-rays preconditioned glasses at indicated doses of 0, 1 and 6 MGy.

The spectra, normalized to the 800 cm^{-1} band, show several features. The main band, peaking at 440 cm^{-1}, is due to a symmetric stretching of oxygens in 6-membered rings [23]. Its shift to higher frequencies confirms a decrease of the interbonding angle Si-O-Si. This shift is about + 5 cm^{-1} for the waveguide written in the pristine, + 10 cm^{-1} for both 1 and 6 MGy samples. It is also accompanied by a shift to lower frequencies of the LO-TO doublet at 1065 cm^{-1} and 1200 cm^{-1}. The most important difference is that the areas under the peaks at 490 cm^{-1} and 605 cm^{-1} (D_1 and D_2 bands) increase confirming a more important densification [24,25] via the generation of lower size more compacted member rings. These bands are

Optical Materials EXPRESS

attributed to breathing motion of bridging oxygen in 4-membered and 3-membered rings respectively. All these changes in the Raman spectra confirm a densification in the silica network and a fs-laser induced positive refractive index change (see the PCM images in the inset in Fig. 3(a), where dark color shows index increase). It also shows the presence of a laser induced band peaking at 900 cm^{-1}, already observed by other authors in samples [26,27] submitted to high radiations doses (γ or neutrons). With a 442 nm excitation, this band is absent, supporting the hypothesis of Di Francesca et al. [27] which associated this band to the Raman resonance of NBOHC.

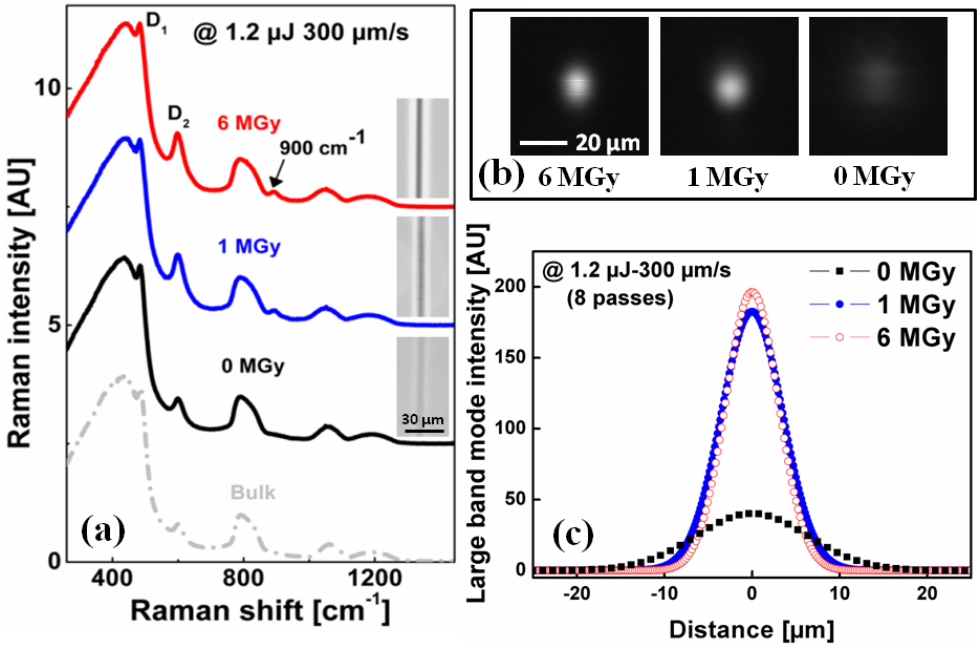

Fig. 3. (a) Raman spectra of three waveguides written with a same dose of laser photons (1.2 µJ-300 µm/s-8 passes) in silica samples pre-irradiated with different X-rays accumulated doses (0 MGy dose corresponds to the pristine sample).The inset gives corresponding PCM images for waveguides written in the 0 MGy (pristine), 1 MGy and 6 MGy samples. The dark color corresponds to a positive index change. The Raman spectra are vertically shifted for better visualization. (b) Large-band guided mode for the waveguide at 1.2µJ-300 µm/s-8 passes in the different pre-irradiated samples. (c) Corresponding large-band mode profile.

The comparison of the samples with different pre-treatment history show several important points. First we can clearly see that the densification is stronger for X-ray preconditioned samples compared to the pristine sample, where the increase in the D_2 bands is almost similar for the 1 and 6 MGy samples. This dose-sensitive densification, induced after exposure to femtosecond laser beam is confirmed for the pretreated glasses in the inset of Fig. 3(a) where PCM images of three waveguides written in a same condition at different accumulated doses of 0 MGy, 1 MGy and 6 MGy are given. We note an increasing contrast of the dark zone shown through the PCM images corresponding to index increase that correlates with the Raman information regarding densification. The white surrounding regions have a less clear origin. They can derive from imaging artefacts as Zernike PCM can generate halos around objects or they can derive from rarefaction regions accompanying the central densification.

Another interesting point is the study of the photo-inscribed waveguides regarding the guided mode. Figure 3(b) shows the large-band guided mode for waveguides written at the same dose of photons (i.e 1.2 µJ-300 µm/s-8 passes) in the different pre-irradiated sample. It is noteworthy to see that the length of these structures is strictly the same (10 mm long)

Optical Materials EXPRESS

whatever the sample. We can clearly see that we have better guiding properties compared with the untreated sample. Moreover, Fig. 3(c) presents the profile of the guided mode confirming, on the one hand, a higher intensity at the output of the waveguide written in the 1 and 6 MGy samples and, on the other hand, a more important mode confinement demonstrated via the measurement of their respective full width at half maximum: 15 µm for the waveguide in the pristine sample and approximately 7 µm for the ones written in the 1 and 6 MGy pre-irradiated samples.

The positive and isotropic Δn allows light guiding. This property can be investigated from near or far field mode measurements. In our case, the Δn measurements of the waveguides was carried out by a butt coupling of white light source into the created waveguide. The far field mode was captured using a CMOS camera and Δn was retrieved based on estimation of the NA of the output light by the relation NA = $\sqrt{2n\Delta n}$. However, this procedure, spectrally averaged over VIS-NIR, is employed for qualitative estimation insofar as it does not give exact Δn distributions. The dependencies of the obtained Δn amplitude in pure silica on the pulse energy and on the scan speeds with 8 passes were measured and the results are displayed in Fig. 4(a). This figure displays the Δn for ultrafast laser written waveguides written at 1.2 µJ with different fs laser scan speeds and for different preconditioning accumulated doses. We can see that for the pristine sample (i.e 0 MGy), Δn remains rather small, with values between 5.10^{-5} and 5.10^{-4}. The same refractive index change is observed even with a 0.5 MGy accumulated dose. However, for the 1 and 6 MGy samples, Δn strongly increase under the same inscription conditions. The reason for the slight Δn decrease when waveguides are written at 100 µm/s can be explained by the creation of a negative refractive index change (Type II) domains meaning that we have reached the Type I/Type II threshold. Through Fig. 4(a), we can clearly see that the material treatment allows having a higher Δn at a same dose of infrared photons. The same trend is observed with a 1.7 µJ pulse energy as shown in Fig. 4(b): the induced Δn seems similar and higher in the 1 and 6 MGy samples compared with the untreated sample where a maximum Δn of roughly 3.10^{-3} is achieved using a scanning speed of 300 µm/s and 8 passes. Writing waveguides below this value induces Type II modifications in the two pre-irradiated samples. We have seen that at a depth of 150 µm corresponding to the localization of the waveguides, a PL intensity of about 364 AU (Arbitrary Unit) and 434 AU for the samples irradiated with a 1 MGy and a 6 MGy X-rays accumulated doses is obtained (see the inset of Fig. 2). Writing a waveguide in those samples at a same depth gives close Δn values. Interestingly, considering that a PL intensity of 364 AU and 434 AU induces a same Δn after laser photoinscription, this technique gives the opportunity to photo-inscribe 3D component with a similar Δn for a depth up to roughly 290 µm by preconditioning the samples with a 6 MGy dose.

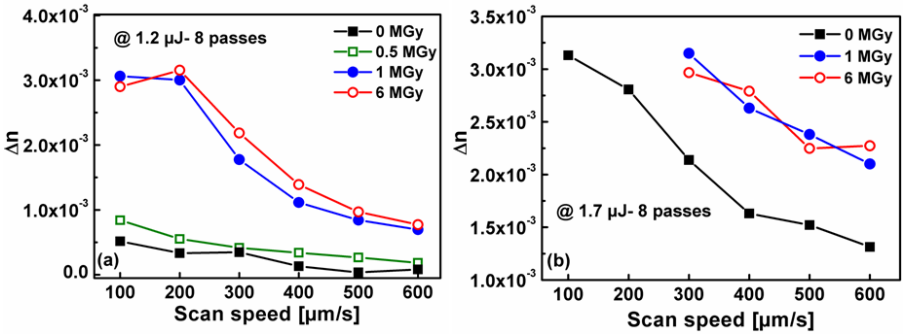

Fig. 4. (a) Variation of refractive index Δn in the ultrafast laser written waveguides versus the scan speed at different X-rays doses (0, 0.5, 1 and 6 MGy). The pulse energy is 1.2 µJ. (b) Variation of Δn versus the scan speed at different X-rays doses (0, 1 and 6 MGy) for a 1.7 µJ pulse.

Optical Materials EXPRESS

The fact that a higher Δn is induced at a same dose of IR photons compared with the pristine sample can be understood based on a model of increased photosensitivity: the multiphotonic ionization (MPI), being the main mechanism of free carrier generation in glass material, can also happens via intermediate states equivalent to an effective reduction of the bandgap. Those virtual states can be caused by defects or impurities. In our case, due to the X-rays pre-treatment, intermediate levels are created thanks to Frenkel pair generation including NBOHC leading to an increase in the absorption capability. As a consequence, the generation of NBOHC serves as precursors for an enhanced photoinscription. However, the procedure of waveguide laser writing involves already the accumulation of a certain number of pulses per micron even in the pristine sample, each of them generating a quantity of defects. That means that at high number of incident pulses the incubation effect was already exploited. This opens up the question why preconditioning with X-rays shows a stronger effect than the standard incubation and defect accumulation process induced by the fs pulses. It is then probable that besides increased photosensitivity, the X-ray preconditioning creates equally a vitreous matrix susceptible of molecular reorganization upon the arrivals of fs pulses.

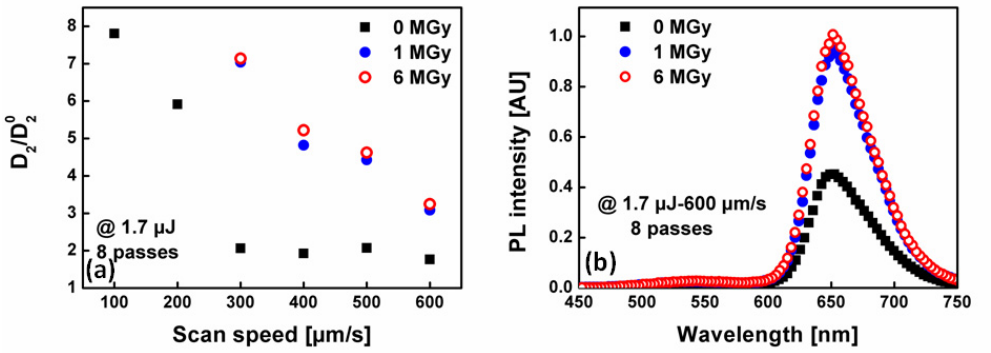

Fig. 5. (a) Relative D_2 areas normalized to the $\mathbf{D_2^0}$ area (before X-ray treatment) at the maximum pulse energy of 1.7 µJ as a function of the scan velocity for different accumulated doses. (b) PL measurements made in three waveguides written in a same condition (i.e 1.7 µJ-600 µm/s) but in the different pre-irradiated samples.

In order to compare the waveguides written in the different samples, we have quantified the structural changes in terms of densification using the D_2 band normalized to the $\mathbf{D_2^0}$ area of the bulk of each sample prior preconditioning and photoinscription. This value highlights the fs-laser induced changes on the amount of 3-membered rings. We apply this method to evaluate the X-ray preconditioning effect for the maximum laser energy allowed to reach a maximum Δn of 3.10^{-3} on the pristine sample before generating Type II modifications, E = 1.7 µJ. Figure 5(a) illustrates the relative D_2 area as a function of the scan speed for waveguides written at 1.7 µJ and 8 passes in samples pre-irradiated with different X-ray doses. It is worth noting that in all samples and for the three doses, its area was found to increase up to a maximum value of roughly 8 times. It is to note that for the 1 and 6 MGy samples, we have reached a Type II modification (negative Δn) for scanning speed of 100 and 200 µm/s. This Type I/ Type II threshold remains similar for these two X-rays doses. Concerning the pristine sample (0 MGy), we observe a very sharp increase in the relative D_2 area when the velocity goes below a value of 300 µm/s. This indicates that the densification becomes less effective for low accumulation number and that the accumulation process becomes nonlinear. At the same time the X-rays preconditioning of the silica near the saturation (1 and 6 MGy) allows having a stronger densification in the waveguides compared with those photoinscribed in the bulk of the pristine sample. The same trend has been

Optical Materials EXPRESS

observed regarding the NBOHC defect accumulation. Figure 5(b) shows the PL yield corresponding to waveguides written at the same dose of photons (1.7 µJ-600 µm/s and 8 passes) but with different precondition doses. Exposure to femtosecond laser in the 1 and 6 MGy samples generate more NBOHC (factor x2) than in pristine sample. We therefore mark a correlation between the increase in the low member rings number, NBOHC yield and Δn.

Interestingly, it is to note that, despite the overall higher efficiency for reaching a high Δn for the preconditioned samples (a higher efficiency per photon), around the value of maximum Δn achievable for fs laser photoinscription, the preconditioning approaches converges to the same maximal densification value. This indicates that a material limit in densification was reached. This high IR photon dose yields a similar Δn in pristine and preconditioned samples, at the limit of a Type I to Type II transition.

4. Conclusion

We have observed the beneficial effect of X-rays preconditioning on the femtosecond laser induced refractive index change in Corning 7980 pure fused silica. This pre-irradiation technique allows for generating precursors defects (NBOHC and E' centers) for further fs-induced defect fabrication inside the bulk but also an increase of the photosensitivity. Based on this pre-treatment, we have maximized the structural changes up to a material densification limit that is intrinsic to the material. Consequently, the preconditioning of the samples with X-rays before the femtosecond laser irradiation increases the achievable refractive index change of the waveguides up to roughly 3.10^{-3} while keeping fs irradiation at lower levels. As we have a higher contrast at a same dose of photons compared with the pristine sample, this preconditioning allows having faster photoinscription processes especially for 3D photonics application. The pre-conditioning effect has equally a fundamental value allowing to validate defect-assistant densification scenarios for the refractive index change.

Funding

LABEX MANUTECH-SISE of Université de Lyon (ANR-10-LABX-0075); The "Investissements d'Avenir" program (ANR-11-IDEX-0007) operated by the French National Research Agency.

References

1. S. Gross and M. J. Withford, "Ultrafast-laser-inscribed 3D integrated Photonics: challenge and emerging applications," Nanophotonics **4**(3), 332–352 (2015).
2. C. D'Amico, G. Cheng, C. Mauclair, J. Troles, L. Calvez, V. Nazabal, C. Caillaud, G. Martin, B. Arezki, E. LeCoarer, P. Kern, and R. Stoian, "Large-mode-area infrared guiding in ultrafast laser written waveguides in sulfur-based chalcogenide glasses," Opt. Express **22**(11), 13091–13101 (2014).
3. J. Martínez, A. Ródenas, T. Fernandez, J. R. Vázquez de Aldana, R. R. Thomson, M. Aguiló, A. K. Kar, J. Solis, and F. Díaz, "3D laser-written silica glass step-index high-contrast waveguides for the 3.5 µm mid-infrared range," Opt. Lett. **40**(24), 5818–5821 (2015).
4. A. Szameit, F. Dreisow, T. Pertsch, S. Nolte, and A. Tünnermann, "Control of directional evanescent coupling in fs laser written waveguides," Opt. Express **15**(4), 1579–1587 (2007).
5. K. Mishchik, C. D'Amico, P. K. Velpula, C. Mauclair, A. Boukenter, Y. Ouerdane, and R. Stoian, "Ultrafast laser induced electronic and structural modifications in bulk fused silica," J. Appl. Phys. **114**(13), 133502 (2013).
6. A. M. Streltsov and N. F. Borrelli, "Study of femtosecond-laser-written waveguides in glasses," J. Opt. Soc. Am. B **19**(10), 2496–2504 (2002).
7. R. Brückner, "Properties and structure of vitreous silica. I," J. Non-Crystal. Solids **5**(2), 123–175 (1970).
8. Y. Cheng, K. Sugioka, K. Midorikawa, M. Masuda, K. Toyoda, M. Kawachi, and K. Shihoyama, "Control of the cross-sectional shape of a hollow microchannel embedded in photostructurable glass by use of a femtosecond laser," Opt. Lett. **28**(1), 55–57 (2003).
9. A. L. Shluger, "The model of a triplet self-trapped exciton in crystalline SiO_2," J. Phys. C Solid State Phys. **21**(13), 431–434 (1988).
10. E. J. Friebele and P. L. Higby, "Radiation effects in amorphous SiO_2 for windows and mirror substrates," in *Laser Induced Damage in Optical Materials: 1987* (H. E. Bannet, 1987).
11. D. M. Krol, "Femtosecond laser modification of glass," J. Non-Cryst. Solids **354** (2–9), 416–424 (2008).

Optical Materials EXPRESS

12. W. Primak, "Mechanism for the Radiation Compaction of Vitreous Silica," J. Appl. Phys. **43**(6), 2745–2754 (1972).
13. R. E. Schenker and W. G. Oldham, "Ultraviolet-induced densification in fused silica," J. Appl. Phys. **82**(3), 1065–1071 (1997).
14. Z. Zheng, J. C. Lambropoulos, and A. W. Schmid, "UV-laser induced densification of fused silica: a molecular dynamics study," J. Non-Crystal. Solids **347**(1–3), 144–152 (2004).
15. L. Zheng, Q. An, R. Fu, S. Ni, and S. N. Luo, "Densification of silica glass at ambient pressure," J. Chem. Phys. **125**(15), 154511 (2006).
16. I. M. Burakov, N. M. Bulgakova, R. Stoian, A. Mermillod-Blondin, E. Audouard, A. Rosenfeld, A. Husakou, and I. V. Hertel, "Spatial distribution of refractive index variations induced in bulk fused silica by single ultrashort and short laser pulses," J. Appl. Phys. **101**(4), 043506 (2007).
17. P. K. Velpula, M. K. Bhuyan, F. Courvoisier, H. Zhang, J. P. Colombier, and R. Stoian, "Spatio-temporal dynamics in nondiffractive Bessel ultrafast laser nanoscale volume structuring," Laser Photonics Rev. **10**(2), 230–244 (2016).
18. L. Skuja, "The origin of the intrinsic 1.9 eV luminescence band in glassy SiO_2," J. Non-Crystal. Solids **179**, 51–69 (1994).
19. L. Skuja, K. Kajihara, M. Hirano, and H. Hosono, "Oxygen-excess-related point defects in glassy/amorphous SiO_2 and related materials," Nucl. Instrum. Methods Phys. Res. B **286**, 159–168 (2012).
20. M. Will, S. Nolte, B. N. Chichkov, and A. Tünnermann, "Optical properties of waveguides fabricated in fused silica by femtosecond laser pulses," Appl. Opt. **41**(21), 4360–4364 (2002).
21. N. Ollier, K. Piven, C. Martinet, T. Billotte, V. Martinez, D. R. Neuville, and M. Lancry, "Impact of glass density on the green emission and NBOHC formation in silica glass: A combined high pressure and 2.5 MeV electron irradiation," J. Non-Crystal. Solids **476**, 81–86 (2017).
22. J. Zhou and B. Li, "Origins of a damaged-induced green photoluminescence band in fused silica revealed by time-resolved photoluminescence spectroscopy," Opt. Mater. Express **7**(8), 2888–2898 (2017).
23. G. S. Henderson, D. R. Neuville, B. Cochain, and L. Cormier, "The structure of GeO_2-SiO_2 glasses and melts: A Raman spectroscopy study," J. Non-Crystal. Solids **355**(8), 468–474 (2009).
24. J. W. Chan, T. Huser, S. Risbud, and D. M. Krol, "Structural changes in fused silica after exposure to focused femtosecond laser pulses," Opt. Lett. **26**(21), 1726–1728 (2001).
25. K. M. Davis, K. Miura, N. Sugimoto, and K. Hirao, "Writing waveguides in glass with a femtosecond laser," Opt. Lett. **21**(21), 1729–1731 (1996).
26. M. León, L. Giacomazzi, S. Girard, N. Richard, P. Martín, L. Martín-Samos, A. Ibarra, A. Boukenter, and Y. Ouerdane, "Neutron irradiation Effects on the structural properties of KU1, KS-4V and I301 Silica Glasses," IEEE Trans. Nucl. Sci. **61**(4), 1522–1530 (2014).
27. D. Di Francesca, A. Boukenter, S. Agnello, A. Alessi, S. Girard, M. Cannas, and Y. Ouerdane, "Resonance Raman of oxygen dangling bonds in amorphous silicon dioxide," J. Raman Spectrosc. **48**(2), 230–234 (2017).